Optical Materials 34 (2011) 461–464

Contents lists available at ScienceDirect

Optical Materials

journal homepage: www.elsevier.com/locate/optmat

Random laser performance of $Nd_xY_{1-x}Al_3(BO_3)_4$ laser crystal powders

S. García-Revilla [a], I. Iparraguirre [a], C. Cascales [b], J. Azkargorta [a], R. Balda [a,c], M.A. Illarramendi [a], M. Al-Saleh [a], J. Fernández [a,c,*]

[a] Departamento Física Aplicada I, Escuela Técnica Superior de Ingeniería, Alda, Urquijo s/n, 48013 Bilbao, Spain
[b] Instituto de Ciencia de Materiales de Madrid-ICMM, CSIC Cantoblanco, 28049 Madrid, Spain
[c] Centro de Física de Materiales CSIC-UPV/EHU and Donostia International Physics Center, Apartado 1072, 20080 San Sebastián, Spain

ARTICLE INFO

Article history:
Received 17 February 2011
Accepted 31 March 2011
Available online 20 May 2011

Keywords:
Laser materials
Random lasers
Multiple scattering

ABSTRACT

We report random laser action in ground powders of $Nd_xY_{1-x}Al_3(BO_3)_4$ ($x = 0.5–1$) laser crystals under nanosecond pulse excitation at 802 nm. The dependence of the random laser threshold energy on the neodymium concentration and focusing conditions is investigated. The slope efficiency of the output random laser emission is determined as a function of Nd^{3+} concentration.

1. Introduction

Systems with strong scattering and gain have been attracting growing attention as a fundamental physical problem at the interface of laser physics, quantum optics, and the mathematical theory of disordered systems. In particular, the interest of this topic arises from the observation of lasing action in a large variety of disordered material structures including highly scattering powders, films, colloidal dye solutions, and human tissues [1–3]. In this type of so called random lasers, the multiple light scattering replaces the standard optical cavity of traditional lasers, and the interplay between gain and scattering determines the lasing properties. A detailed discussion of the latest results and theories concerning the mechanisms responsible for random lasing and the precise nature of the random laser modes can be found in Refs. [1,4–6].

Since 1986 when Markushev et al. demonstrated laser-like behaviour in a powder of $Nd_5La_{1-x}(MoO_4)_4$ at liquid nitrogen temperature [7], similar random laser experiments have been conducted at room temperature in numerous Nd-doped pulverized materials, mixtures of these powders, and highly scattering Nd-doped ceramics. The history and the state of the art of these neodymium-activated random lasers are reviewed in Ref. [2]. Among them, the $NdAl_3(BO_3)_4$ powder is regarded as a promising solid-state random laser material [8]. Note that the neodymium aluminium borate has many desirable features, such as a low laser threshold, a high gain, high Nd^{3+} concentration, and excellent physical and chemical properties [9]. Nevertheless, it is extremely difficult to grow single crystals of high optical quality and large enough for cutting them into laser rods. Common features to pulsed neodymium random lasers such as a dramatic shortening of the emission pulse, a narrowing of the emission spectral line, and the appearance of relaxation oscillations above a critical energy value were already found in $NdAl_3(BO_3)_4$ powder by Noginov et al. [10]. These authors also performed quantitative measurements of the random laser parameters of materials of similar families such as $Nd_{0.5}La_{0.5}Al_3(BO_3)_4$, $NdSc_3(BO_3)_4$, and $Nd_{0.5}La_{0.5}Sc_3(BO_3)_4$ as a function of the particle size and of the pumped spot size [11–13]. In addition, coherence studies based on interferometric measurements and speckle pattern analysis, as well as theoretical modelling of the experimental random laser results within the diffusion approximation, were carried out in these scattering media [2]. On the other hand, in previous papers we have determined, the transport-mean-free path (l_t) of $NdAl_3(BO_3)_4$ and $Nd_xY_{1-x}Al_3(BO_3)_4$ laser crystal powders by using the diffuse reflectance and transmittance of the powders and the absorption coefficient of the crystal materials [14,15]. It is important to note that the knowledge of this parameter is very important to understand the operation regime of random lasers. Here, we study the random laser performance of ground powders of the yttrium borate family, $Nd_xY_{1-x}Al_3(BO_3)_4$ ($x = 0.5–1$). The dependence of their random laser threshold, slope efficiency, and emission kinetics on the Nd^{3+} concentration is investigated. Although the observed phenomena are qualitatively similar in all the explored powders, our findings show a reduction of the onset of laser-like emission and an increase of the slope efficiency when increasing the Nd^{3+} content. In addition, we have experimentally studied the dependence of

* Corresponding author at: Departamento Física Aplicada I, Escuela Técnica Superior de Ingeniería, Alda, Urquijo s/n, 48013 Bilbao, Spain.
E-mail address: wupferoj@bi.ehu.es (J. Fernández).

0925-3467/$ - see front matter © 2011 Published by Elsevier B.V.
doi:10.1016/j.optmat.2011.03.047

the pump energy density at threshold on the pumped area in both the $NdAl_3(BO_3)_4$ and $Nd_{0.5}Y_{0.5}Al_3(BO_3)_4$ laser crystal powders.

2. Experimental

Polycrystalline powders of $Nd_xY_{1-x}Al_3(BO_3)_4$ ($x = 0.5$, 0.6, 0.7, 0.8, 0.9, and 1) have been prepared from citrate precursors obtained by the soft chemistry procedures given in [15]. Rhombohedral R32 crystal structure and purity of the samples were tested by X-ray diffraction analysis at room temperature using a Bruker D-8 diffractometer with Cu Kα radiation. The laser materials were subsequently ground by using a mixer mill. The polydispersity of the resulting powder was evaluated from SEM (scanning electron microscope) photographs. As an example, Fig. 1 shows the particle size histogram of the $Nd_{0.9}Y_{0.1}Al_3(BO_3)_4$ laser crystal powder. Fitting the histogram to a log-normal function we obtained an average particle size of 4 ± 2 μm, that is similar for all samples. All the ground powder samples were compacted in quartz cells without a front window for handling ease and optical characterization. The volume filling factor of the powder materials ($f = 0.39$) was calculated by measuring sample volume and weight.

The random laser experiments were performed at room temperature in a backscattering arrangement by using a Ti-sapphire laser pumped by a pulsed frequency doubled Nd: YAG laser (9 ns pulse width) as the excitation source. The pump beam diameter on the sample surface was varied from 0.3 to 4 mm. The emission from the front face of the samples was collected with an optical fibre. A long-pass filter was used to remove light at the pump wavelength (802 nm). In the spectral measurements, the emitted light was dispersed by a 0.25 m monochromator and detected with a photomultiplier coupled to a boxcar integrator. The emission kinetics traces were recorded by using a fast photodiode (Thorlabs SIR-5) connected to a digital oscilloscope (temporal resolution of 400 ps).

3. Results and discussion

We experimentally analysed the spectra and emission dynamics of $Nd_xY_{1-x}Al_3(BO_3)_4$ ground powders when increasing the excitation energy. At low pumping energies, these laser crystal powders show only regular spontaneous emission with a single exponential emission kinetics. Table 1 displays the lifetime dependence of the Nd^{3+} upper laser level, $^4F_{3/2}$, on the rare earth concentration. Fig. 2 shows in red the normalized spontaneous emission spectrum of the $NdAl_3(BO_3)_4$ powder at the $^4F_{3/2} \rightarrow {}^4I_{11/2}$ transition. This spectrum was measured at 4 m J/pulse, with a pump beam diameter on the sample of 1.87 mm. On the other hand, with the increase of the pumping energy, the amplified spontaneous emission of the laser crystal powders increases causing an enhancement of the emission intensity and a non exponential nature of the emission dynamics. In particular, above a certain critical threshold value both the spectra and the kinetics of Nd^{3+} luminescence change dramatically. The intensity of the strongest line in the spontaneous emission spectrum increases several orders of magnitude and its width becomes smaller. As evidenced in Fig. 2, the spectrum collapses to a narrow single line with a linewidth of 0.4 nm. The blue curve of this plot centered at 1064 nm, corresponds to the emission spectrum of the $NdAl_3(BO_3)_4$ powder obtained at 20 m J/pulse. It is worthy to remark that no spikes were observed in the laser-like emission spectra of our powder samples which suggests a nonresonant feedback mechanism of the explored random laser effect.

As mentioned before, just above the threshold energy the emission kinetics changes to a very short and intense emission pulse with a duration in the nanosecond time-scale (~1 ns). At stronger pumping, a second emission pulse emerges in the kinetics, and as the pumping energy is increased, the number of stimulated emission pulses increases manifesting the typical laser relaxation behaviour. Notice that relaxation oscillations in random lasers have been theoretically predicted by Letokhov in 1968 [16] and studied more recently in detail [17] and references therein. In neodymium random lasers, they occur in a highly nonlinear regime showing narrow stimulated emission pulses (~1 ns) occurring during a much longer pumping pulse (~10 ns) [10]. These oscillations are strong in the beginning of the lasing process and are damped at longer times. Moreover, the study of the kinetics of relaxation oscillations in random lasers reveals information about the photon residence time in the scattering medium [13]. Fig. 3 shows the temporal evolution of the $NdAl_3(BO_3)_4$ powder emission recorded below the lasing threshold (2 m J/pulse red line), just above the lasing threshold (5 m J/pulse green line), and well above the lasing threshold (15 m J/pulse blue line) with the same pump spot size used to measured the emission spectra. As can be observed, the delay time between the first emission pulse and the onset of the fluorescence becomes shorter as the excitation energy increases. The other laser crystal powders exhibited a qualitative similar behaviour.

We also explored the dependence of the random laser threshold energy of the $NdAl_3(BO_3)_4$ and $Nd_{0.5}Y_{0.5}Al_3(BO_3)_4$ laser crystal powders on the size of the pumped spot. Fig. 4 depicts the threshold pumping density of both samples as a function of the pumped area. Both curves show the same behaviour but larger threshold values are found in the non-stoichiometric borate powder. As can be observed, the threshold pumping density sharply increases at rather

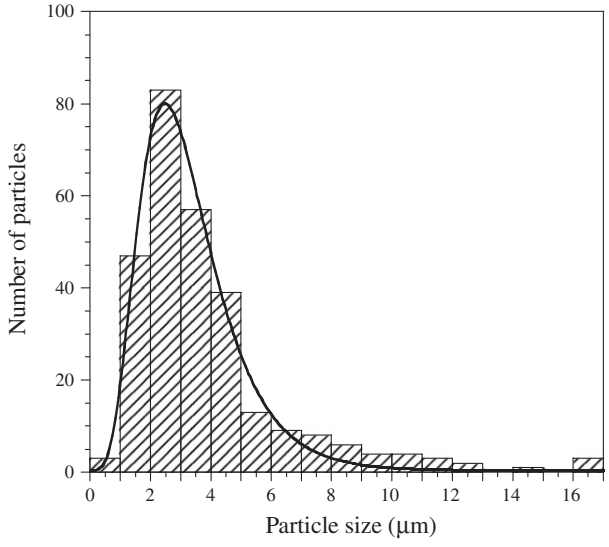

Fig. 1. Particle size histogram of the $Nd_{0.9}Y_{0.1}Al_3(BO_3)_4$ powder. The solid line is the log-normal fit from which the average particle size is calculated.

Table 1
Lifetime values of the $^4F_{3/2}$ Nd^{3+} upper laser level in the $Nd_xY_{1-x}Al_3(BO_3)_4$ ($x = 0.5$–1) powders ($\lambda_{exc} = 802$ nm).

x (Nd^{3+} content)	$\tau_{^4F_{3/2}}$ (μs)
0.5	15.6
0.6	14.7
0.7	13.6
0.8	12.8
0.9	12.5
1.0	12.7

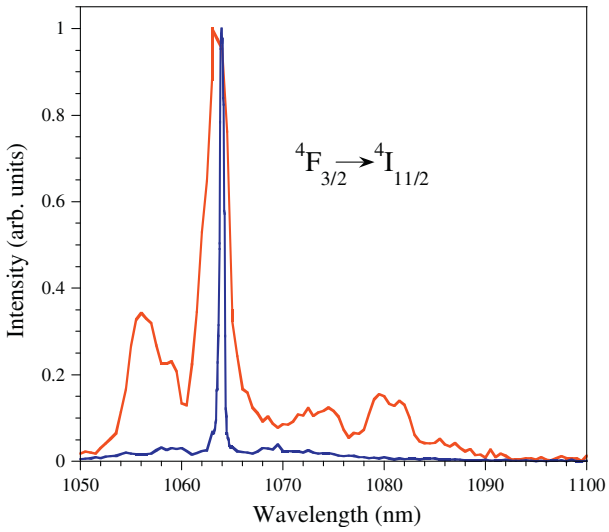

Fig. 2. Normalized emission spectra of the $NdAl_3(BO_3)_4$ powder obtained by pumping at 802 nm with a pump spot size of 1.87 mm. The red and blue lines correspond to the fluorescence and laser-like emission spectra measured below and above the threshold at 4 m J/pulse and 20 m J/pulse, respectively. (For interpretation of the references to colour in this figure legend, the reader is referred to the web version of this article.)

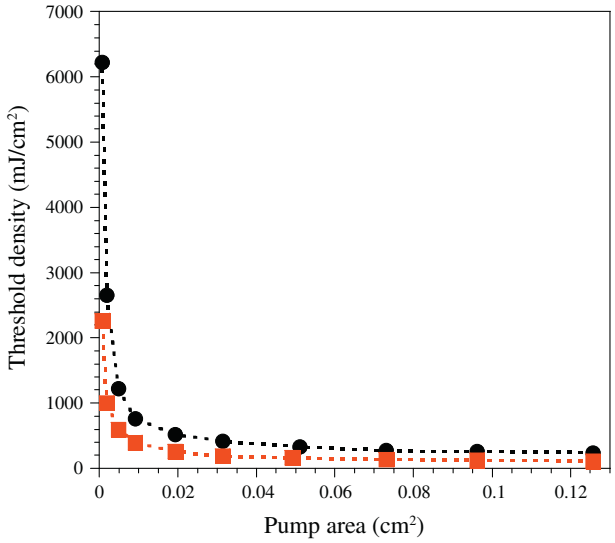

Fig. 4. Threshold pumping density of the $NdAl_3(BO_3)_4$ (red squares) and $Nd_{0.5}Y_{0.5}Al_3(BO_3)_4$ (black dots) powders as a function of the pumped spot area (λ_{exc} = 802 nm). (For interpretation of the references to colour in this figure legend, the reader is referred to the web version of this article.)

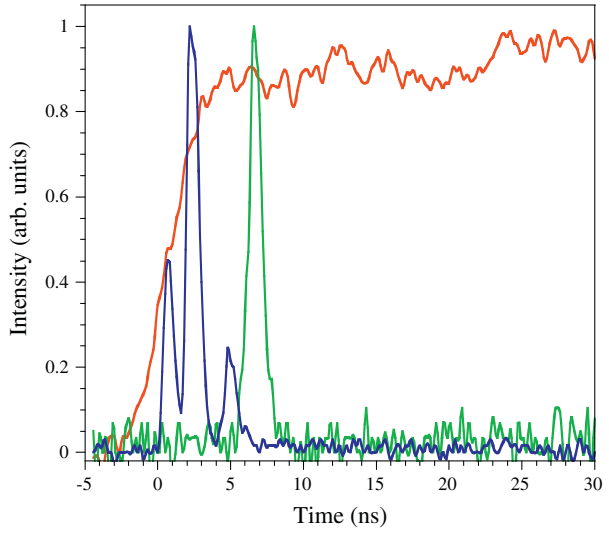

Fig. 3. Temporal evolution of the emission intensity of the $NdAl_3(BO_3)_4$ powder obtained at 2 m J/pulse (red line), 5 m J/pulse (green line), and 15 m J/pulse (blue line) with a pump spot size of 1.87 mm (λ_{exc} = 802 nm). (For interpretation of the references to colour in this figure legend, the reader is referred to the web version of this article.)

small areas of the pumped spot (where damage of the powder laser material can also occur at high pumping energies). In order to explain this result, one should take into account that (1) gain spatial distribution is governed by the spreading of pump light in the powder, and (2) light is emitted in the pumped region of the powder from where it starts to diffuse. For small excitation beam sizes, the light paths will very probably leave the amplifying or pumped volume after a short time, with a small chance to return. This implies that the threshold pumping density should be high as a large gain is needed to compensate losses. With the increase of the size of the pumped spot, the amplifying volume increases. Therefore, photon walk paths elongate as light can travel longer inside the gain volume and can be more strongly amplified. Furthermore, if the photon leaves the gain volume and reaches the passive (unexcited) part of the powder, it could have a higher chance to return back to the amplifying region because of the larger excited volume. Consequently, a reduction of the random laser threshold density is expected in such a case. Nevertheless, as evidenced from Fig. 4, the threshold pumping density is almost independent of the pump spot area at large diameters. This behaviour can be explained regarding the flat-disk geometry of our pumping (the pump beam diameter, d, is larger than the penetration depth, which is typically less than 60 μm in neodymium random lasers at 532 nm [13]). Note that as $d \rightarrow \infty$ the number of paths per unit area of the pumped spot with a greater enough length to produce laser-like emission does not increase infinitely, but rather it will saturate at some constant value accounting for the saturation behaviour presented in Fig. 4 [11]. The same threshold trend with the pump beam size was experimentally observed in other neodymium doped materials [11]. It is worthy mentioning that the condition for the diffusion approximation ($\lambda \ll l_t \ll L$, where λ is the pump wavelength and L is the scattering sample thickness) is satisfied in the explored powder samples as l_t was estimated to be around 9.3 μm in the $NdAl_3(BO_3)_4$ and non-stoichiometric powders at the excitation wavelength (λ = 802 nm).

It is also clear from Fig. 4 that the Nd^{3+} concentration strongly influences the onset of laser-like emission. By measuring the input–output curves of the $Nd_xY_{1-x}Al_3(BO_3)_4$ laser crystal powders, we studied the Nd^{3+} concentration effect on the random laser performance of this yttrium borate family. Fig. 5 shows the time integrated output intensity of the random laser pulses versus pump pulse energy for Nd^{3+} concentrations between x = 0.5 and 1. A pump spot size of 2 mm was employed. As already mentioned, just above the threshold the emission intensity undergoes a dramatic increase which is linear with pump fluence making the threshold sharp and well defined. As in regular lasers, the linear fit of these curves provides not only the threshold value but also the slope efficiency of stimulated emission. The fits corresponding to each powder sample are also displayed in Fig. 5. Fig. 6 shows the random laser threshold energies (blue squares) and slopes (green diamonds) inferred from the linear fits of the experimental data depicted in Fig. 5. The red points of Fig. 6 represent the critical energy value at which the emission kinetics of the different

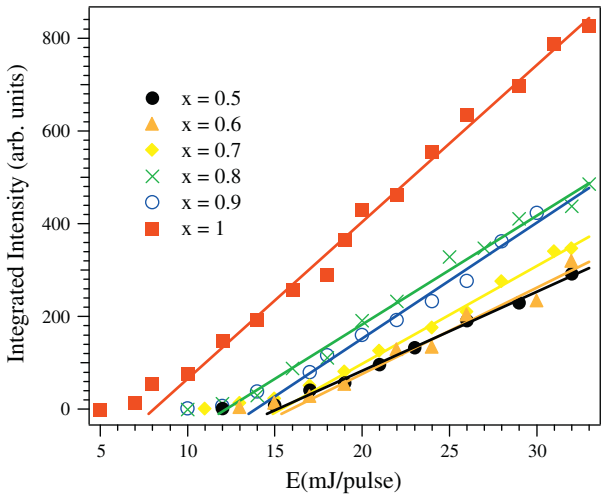

Fig. 5. Time integrated intensity of the output pulses of $Nd_xY_{1-x}Al_3(BO_3)_4$ (x = 0.5–1) powders as a function of the pump energy. Black dots, orange triangles, yellow diamonds, green crosses, blue circles, and red squares correspond to powder compositions with x = 0.5, 0.6, 0.7, 0.8, 0.9, and 1, respectively. Solid lines represent the linear fits of the experimental data. The diameter of the pump spot is 2 mm (λ_{exc} = 802 nm). (For interpretation of the references to colour in this figure legend, the reader is referred to the web version of this article.)

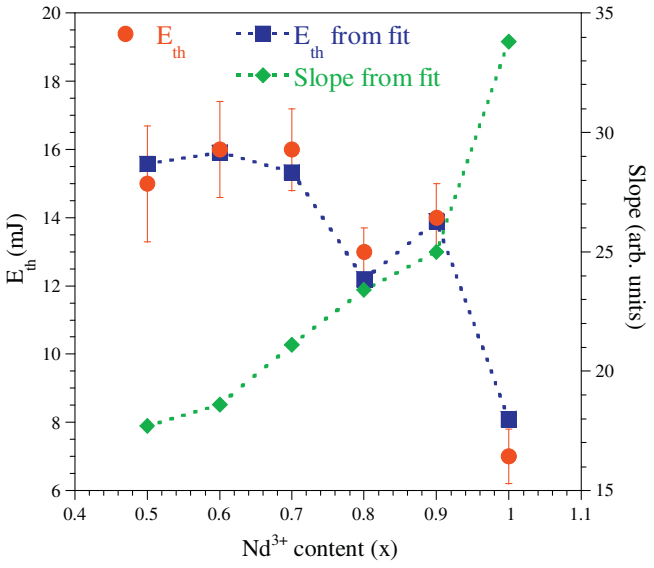

Fig. 6. Random laser threshold energy (blue squares) and relative slope (green diamonds) values obtained from the linear fits of the input–output curves of the $Nd_xY_{1-x}Al_3(BO_3)_4$ powders as a function of the Nd^{3+} content. Red dots correspond to the energy values at which their emission dynamics is shortened to one short pulse. The error bars represent the energy fluctuations of the pump laser. (For interpretation of the references to colour in this figure legend, the reader is referred to the web version of this article.)

powder samples is shortened to one short pulse. The error bars of these data are due to the energy fluctuations of the Ti-sapphire pump laser. As expected, there is a good agreement between these energies and the threshold values obtained from the linear fit of the input–output curves (blue squares). It is clear from Fig. 6 that despite the existence of some lifetime concentration quenching (see Table 1), the increase of the Nd^{3+} content in the yttrium borate family leads to a reduction of the random laser threshold and to an enhancement of the relative slope of the random laser emission. Note that under the focusing conditions described above, the threshold energy of the $Nd_{0.5}Y_{0.5}Al_3(BO_3)_4$ powder is about 15 m J/pulse whereas the onset of laser-like emission in the $NdAl_3(BO_3)_4$ powder is around 7 m J/pulse. Moreover, the stoichiometric powder has twice a larger slope efficiency than the former one.

4. Conclusions

Random laser-like effects such as spectral narrowing and pulse shortening have been observed and characterized in the ground powder of $Nd_xY_{1-x}Al_3(BO_3)_4$ (x = 0.5–1) laser crystals. We have presented an experimental study of the dependence of the onset of stimulated emission on the focused pump beam area. It has been found that the decrease of the pump beam diameter leads to an increase of the random laser threshold density. On the other hand, our results clearly demonstrate that despite the existence of some lifetime concentration quenching, one can optimize the output of stimulated emission and minimize the threshold energy by increasing the Nd^{3+} content of the laser crystal powders. In particular, the $NdAl_3(BO_3)_4$ powder, which is the most efficient one, has a threshold energy of around 7 m J/pulse (with a pump beam size of 2 mm).

Acknowledgments

This work has been supported by the Spanish Government MEC under Projects No. MAT2008-05921/MAT, Consolider SAUUL CSD2007-00013, and Basque Country Government (IT-331-07).

References

[1] D.S. Wiersma, Nat. Phys. 4 (2008) 359–367.
[2] M.A. Noginov, Solid-State Random Lasers, Springer, Berlin, 2005.
[3] H. Cao, Waves Random Media 13 (2003) R1–R39.
[4] D.S. Wiersma, M.A. Noginov, J. Opt. 12 (2010) 020201.
[5] J. Fallert, R.J.B. Dietz, J. Sartor, D. Schneider, C. Klingshirn, H. Kalt, Nat. Photon. 3 (2009) 279–282.
[6] J. Andreasen, A.A. Asatryan, L.C. Botten, M.A. Byrne, H. Cao, L. Ge, L. Labonté, P. Sebbah, A.D. Stone, H.E. Türeci, C. Vanneste, Adv. Opt. Photon. 3 (2011) 88–127.
[7] V.M. Markushev, V.F. Zolin, C.M. Briskinia, Sov. J. Quantum Electron. 16 (1986) 281–283.
[8] M. Bahoura, M.A. Noginov, J. Opt. Soc. Am. B 20 (2003) 2389–2394.
[9] D. Xue, S. Zhang, J. Phys.: Condens. Matter 8 (1996) 1949–1956.
[10] M.A. Noginov, N.E. Noginova, H.J. Caulfield, P. Venkateswarlu, T. Thompson, M. Mahdi, V. Ostroumov, J. Opt. Soc. Am. B 13 (1996) 2024–2033.
[11] M. Bahoura, K.J. Morris, M.A. Noginov, Opt. Commun. 201 (2002) 405–411.
[12] M.A. Noginov, G. Zhu, A.A. Frantz, J. Novak, S.N. Williams, I.N. Fowlkes, J. Opt. Soc. Am. B 21 (2004) 191–200.
[13] M. Bahoura, K.J. Morris, G. Zhu, M.A. Noginov, IEEE J. Quantum Electron. 41 (2005) 677–685.
[14] M.A. Illarramendi, I. Aramburu, J. Fernández, R. Balda, M.A. Noginov, Opt. Mater. 27 (2005) 1686–1691.
[15] M.A. Illarramendi, C. Cascales, I. Aramburu, R. Balda, V.M. Orera, J. Fernández, Opt. Mater. 30 (2007) 126–128.
[16] V.S. Letokhov, Sov. Phys. JETP 26 (1968) 835–840.
[17] G. Zhu, T. Tumkur, M.A. Noginov, Phys. Rev. A 81 (2010) 065801.